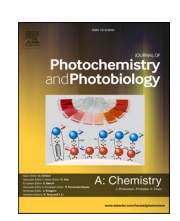


Contents lists available at ScienceDirect

Journal of Photochemistry & Photobiology, A: Chemistry

journal homepage: www.elsevier.com/locate/jphotochem





Photometric sensing of heavy metal ions using a naphthoquinodimethyl-*bis*-thioamide dye: Selectivity & photophysics of the metal organic complexes

Samjhana Maharjan ^{a,b}, Young Ju Yun ^{a,b,1}, Veronica A. Okello ^{c,2}, Gary P. Wiederrecht ^{d,4}, David J. Gosztola ^{d,3}, A. Jean-Luc Ayitou ^{a,b,5,*}

- ^a Department of Chemistry, Illinois Institute of Technology, Chicago, IL 60616, United States
- ^b Department of Chemistry, University of Illinois at Chicago, Chicago, IL 60607, United States
- ^c Department of Physical Sciences, Machakos University, P.O Box 136-90100, Machakos, Kenya
- ^d Center for Nanoscale Materials, Argonne National Laboratory, Lemont, IL 60439, United States

ARTICLE INFO

Keywords: Molecular sensors Heavy metal pollutants Photoluminescence Photophysics

ABSTRACT

As Mother Nature is experiencing catastrophic environmental pollutions from both natural sources and anthropogenic activities, many scientists have been working around the clock to develop environmentally benign and cost-effective, yet sensitive, detection techniques for pollutants, especially heavy metal species (e.g. lead, cadmium, mercury, among others) that are deleterious to human health. Herein, we report a novel sulfurcontaining small organic dye/sensor naphthoquinodimethyl-bis-thioamide (QDM), which was found to be particularly selective toward mercury ion (Hg²⁺). Using a combination of UV-vis absorption, photoluminescence, and time-resolved pump-probe techniques, we established that QDM and Hg²⁺ can form stable complex(es) due to the strong affinity of sulfur toward mercury. In this investigation, while a higher ratio of QDM:Hg²⁺ was necessary to fully quench the fluorescence emission of QDM, only 1 equiv of the Hg²⁺ ion was necessary to observe the sensing effect on the excited state photo-behavior(s) of QDM. The present results highlight a synergy between molecular sensors' selectivity/sensitivity and sensor-analytes dynamics.

1. Introduction

Heavy metal pollutants such as lead, arsenic, chromium, mercury, cadmium, among others have been declared human carcinogens by the U.S. Environmental Protection Agency and the International Agency for Research on Cancer [1]. Although these heavy metal species can occur naturally (from volcanoes and geothermal activities), the main environmental sources of these pollutants are anthropogenic, such as coal combustion, waste incineration, metal mining, petroleum refining and manufacturing, and chlorine-alkali production [2]. Interestingly, not all metal ions (M^{n+}) are deleterious to human health; it has been reported that low quantities of chromium, copper, manganese, iron, and zinc for

example are essential nutrients for humans [3]. While large quantities of these metals would undoubtedly become hazardous to humans and other living organisms [4], trace amounts of mercury (in the form of salts or organo-complexes) can cause a severe health risk for humans [5–7]. Mercury salts such as HgCl₂ and organo-mercury compounds like MeHg [8] can cause mercurial stomatitis, loosening of the teeth, renal damage, and neurological damage. Furthermore, tremors, depression, and behavioral disturbances are the consequence of inhalation of metallic mercury vapor [9].

Fortunately, several analytical tools/techniques are available for heavy metal detection, in the environment. Flame photometry [10], atomic absorption spectrometry [11,12], ion-sensitive electrodes [13],

^{*} Corresponding author at: Department of Chemistry, University of Illinois at Chicago, Chicago, IL 60607, United States. E-mail address: aayitou@uic.edu (A.J.-L. Ayitou).

¹ ORCID: 0000-0002-8612-4244.

² ORCID: 0000-0002-7766-1822.

³ ORCID: 0000-0003-2674-1379.

⁴ ORCID: 0000-0001-8821-932X.

⁵ ORCID: 0000-0001-6355-2564.

$$\begin{array}{c} C_8H_{17} \\ \hline \\ C_8H_{17} \\ \hline \\ ACN \\ \hline \\ C_8H_{17} \\ C_8H_{17} \\ \hline \\ C$$

Scheme 1. Sensing/complexation of heavy metal analytes using QDM. Species/complexes I and II interconvert in the medium depending on the concentration of the metal ion analytes.

electron microprobe analysis [14,15], and neutron activation analysis [16] are some of the modern-day techniques which are routinely used and well-documented for the detection of heavy metal/metallic ion pollutants. Although these detection techniques have high selectivity and sensitivity, they may require expensive tools/setup/instrumentation as well as a large sample size; in addition, these analytical tools/ techniques do not allow continuous monitoring-they can also require routine calibration and maintenance. In furtherance, several low-cost, yet sensitive alternatives have been developed in recent years. The photometric technique is one such alternative [17]. In this method, suitable molecules or molecular sensors (with characteristic photoluminescence emission) are employed and their emission is either quenched or enhanced in the presence of the toxic metal analytes. Hence, the change in emission intensity and/or the lifetime of the emission band becomes a benchmark detection technique of the heavy metal analytes. Herein, we report a sulfur-containing naphthoquinodimethyl-bis-thioamide (QDM) as a novel visible light absorbing dye/sensor with characteristic photoluminescence/photophysical properties, which can be tailored for the detection of toxic metal pollutants in the environment (Scheme 1).

QDM was first developed and fully characterized in our lab [18]. Based on its UV–vis absorption and emission characteristics, it was found that **QDM** absorbs visible photons up to ca. 580 nm. Upon visible light-excitation, **QDM** fluoresces with an emission maximum centered at ca. 545 nm (in ACN) and a quantum yield $\Phi_{Fl}=0.2\%$ (in DCM). Due to this low Φ_{Fl} value, we were able to establish that **QDM** can phosphoresce in the 700–850 nm window with a lifetime $\tau_{phos}=0.3$ –0.4 ms [19,20]. As noted earlier, the structure of **QDM** also features thio-carbonyl groups which can be exploited as binding site(s) with the metal analytes of interest. Particularly, we hypothesize that the sulfur atom(s) may induce high binding affinities of **QDM** with the aforementioned $\mathbf{M}^{\mathbf{n}+}$ ions.

In the present work, a combination of UV–vis absorption, photo-luminescence, and time-resolved pump–probe (TA) spectroscopy methods have been employed to unravel the sensing ability of **QDM** in the presence of $\mathbf{As^{3+}}$, $\mathbf{Cd^{2+}}$, $\mathbf{Cr^{3+}}$, $\mathbf{Hg^{2+}}$, $\mathbf{Pb^{2+}}$, and $\mathbf{Sn^{2+}}$. Specifically, strong interactions upon the addition of $\mathbf{Hg^{2+}}$ to a sample of **QDM** was expected [21], since it has been documented that sulfur and $\mathbf{Hg^{2+}}$ would form stable complexes [22–24]. Hence, **QDM** would exhibit a unique selective/affinity in the presence of $\mathbf{Hg^{2+}}$ ions (mercury-containing samples).

2. Materials and Methods

All commercially obtained metal salts were used immediately after their purchase without further purification. All solvents used in these experiments were of spectroscopy grade. Fresh samples of **QDM** were prepared using purified/recrystallized materials. Stock solutions each of the analytes $\mathbf{M}^{\mathbf{n}+}$ (concentration) were prepared in ACN for \mathbf{HgCl}_2 (0.37 M) and \mathbf{SnCl}_2 (0.0072 M), in EtOH for \mathbf{CrCl}_3 (0.0076 M), \mathbf{AsI}_3 (0.0073 M), and \mathbf{CdCl}_2 (0.0082 M), and in DMF for \mathbf{PbCl}_2 (0.0078 M).

UV–vis absorption spectra were recorded using an Ocean Optics spectrometer (DH-MINI UV–Vis -NIR light source) equipped with a QE-Pro detector; for each metal analytes, the initial sample optical density (O.D.) for **QDM** is 0.2 at $\lambda_{Exc}=470$ nm. However, the fluorescence emission spectra were recorded with samples of O.D. = 0.1 at $\lambda_{Exc}=470$ nm on an Edinburgh Instrument spectrofluorometer FLS980.

Time-resolved pump-probe spectroscopy was performed using an amplified Ti:sapphire laser system (Spectra-Physics Spitfire) equipped with an optical parametric amplifier (OPA, Light Conversion, TOPAS). This system produces 130 fs pulses at 5 kHz centered at 800 nm. 95% of the output from the amplifier is directed to the OPA to generate tunable pump pulses in the visible and near-infrared spectral regions. For operation with 130 fs temporal resolution, the pump pulse and the remaining 5% of output from the amplifier are directed to a transient absorption spectrometer (Helios from Ultrafast Systems), where the 5% output is used to generate a continuum probe pulse extending from 450 nm to 1400 nm by focusing into a thin sapphire window. The pump pulse is chopped at half the repetition rate to measure a difference spectrum for the transient absorption measurement. The incident pump pulse for these experiments at 470 nm had energy on the sample of 300 nJ per pulse, focused to a 200-μm-diameter spot. The transmitted probe light was collected and fiber optically coupled to a spectrograph that used a visible (Si) array detector. Data were collected for continuum wavelengths from 450 nm to 750 nm as a function of delay track position for the continuum probe relative to the undelayed pump pulse. The temporal chirp of the data was experimentally determined and corrected before analysis. For longer time scale processes, the probe light comes from a continuum light source (EOS from Ultrafast Systems). In this case, the system operates at 1 kHz and has a time resolution of 200 ps/point. Decay times of several hundred microseconds can be measured.

NMR titrations were performed in acetone-d₆ using a 300 MHz

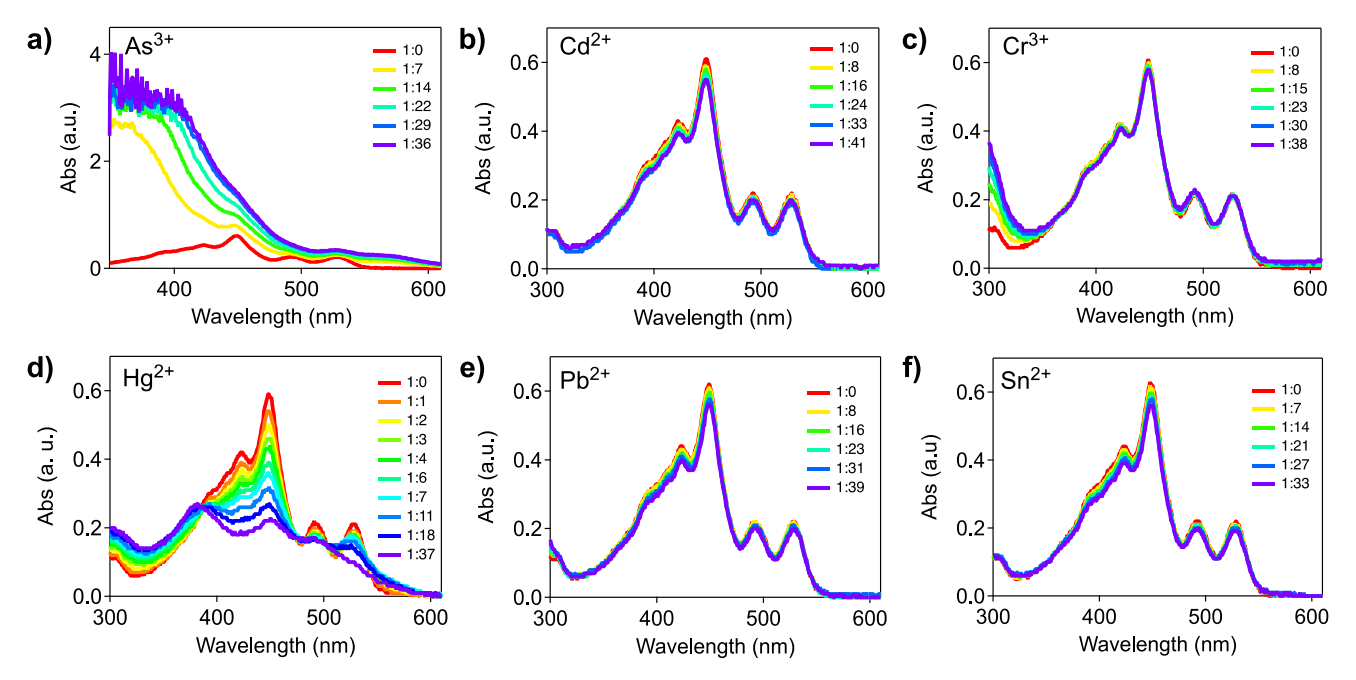


Fig. 1. UV-vis absorption spectra of QDM recorded in ACN in the presence of the M^{n+} at various equivalents (concentrations).

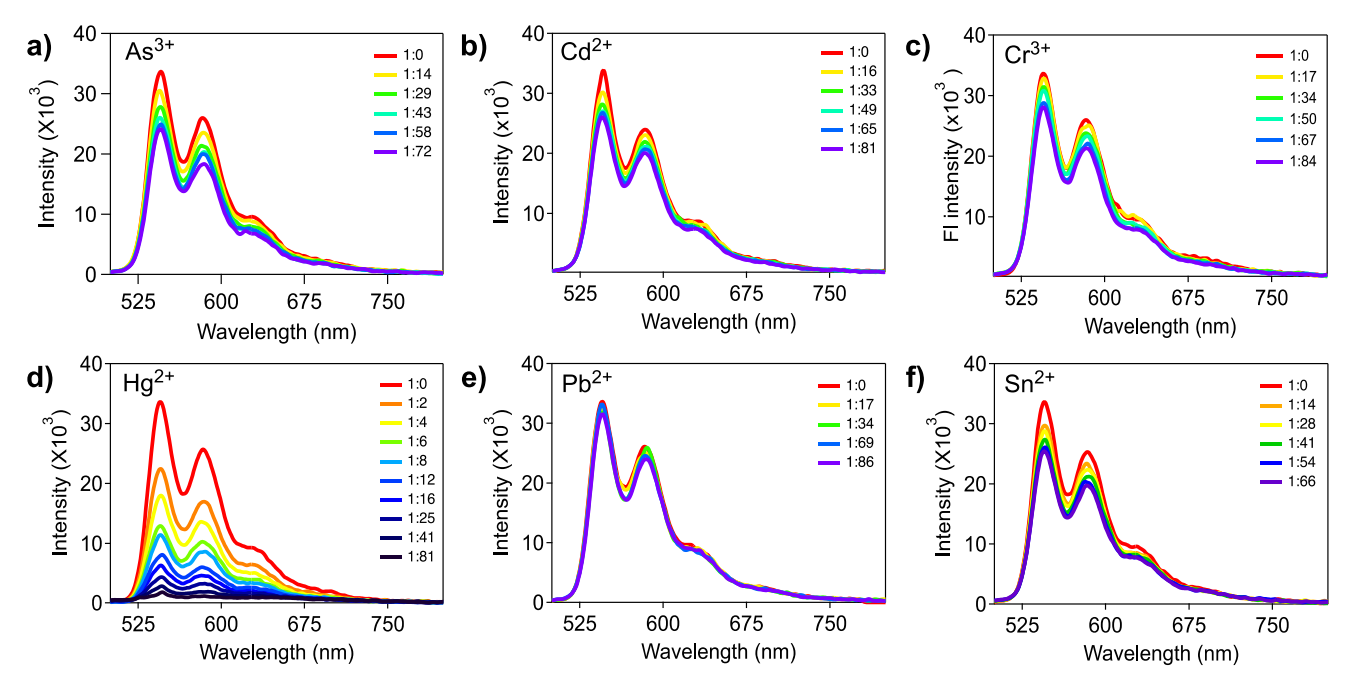


Fig. 2. Fluorescence emission spectra of QDM in the presence of the M^{n+} at various equivalents (concentrations): sample O.D. = 0.1 at $\lambda_{Exc} = 470$ nm. The spectra were recorded in ACN.

Bruker spectrometer.

3. Results & Discussions

3.1. UV-vis absorption spectroscopy

As Fig. 1a–f reveals, the absorption profiles of QDM in acetonitrile (ACN) changed upon gradual addition of aliquots of M^{n+} (As^{3+} , Cd^{2+} , Cr^{3+} , Hg^{2+} , Pb^{2+} , and Sn^{2+}). Except for As^{3+} , which exhibits additive/complementary absorption besides the intrinsic absorption of QDM, the presence of all other ions in the samples of QDM did show changes in the intensity of the QDM profile. While the addition of Cr^{3+} led to the least

change in the absorption profile (Fig. 1c), the magnitude and shape/transitions of the absorption of **QDM** changed when higher equivalents of Hg^{2+} were added to the solution (Fig. 1d). The significant changes in the absorption of **QDM** in the presence of Hg^{2+} (and to some extent Cd^{2+}) are suggestive of covalent or non-covalent interactions (in the form of sulfur atom··· M^{n+} complex) between **QDM** and solvated mercury/cadmium ions, as shown in Scheme 1. It is important to note that the decrease or change in the absorption profile of **QDM** in the presence of 10-20 equiv of Hg^{2+} features a broadening of the main transitions at ca. 450-530 nm. We hypothesize that this significant change is reminiscent of charge transfer (LMCT C = S····Hg) in [**QDM-Hg**²⁺] species or complexes [25-27].

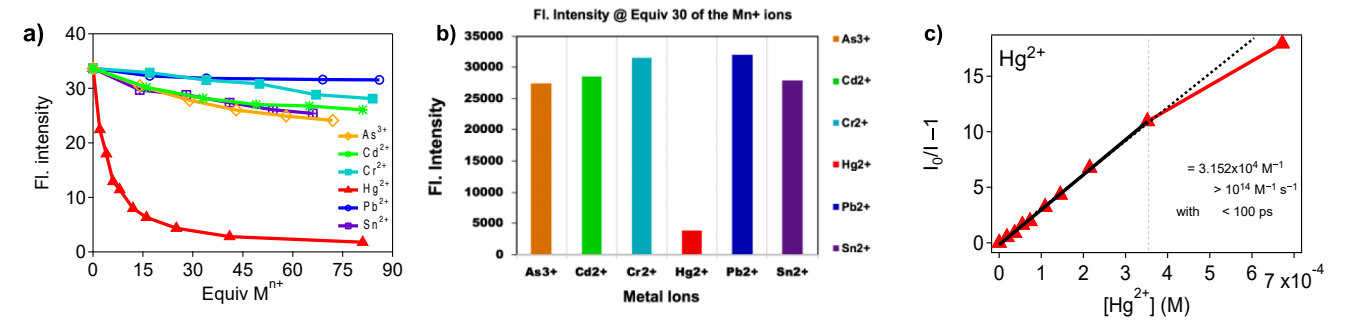


Fig. 3. a) Selectivity of QDM toward the M^{n+} ions using the fluorescence emission intensities of QDM. b) Selectivity at 30 equiv of the M^{n+} ions. c) Stern-Volmer quenching of QDM's fluorescence band by Hg^{2+} ion showing a dynamic QDM... Hg^{2+} interaction beyond ca. 30 equiv of Hg^{2+} .

3.2. Quenching of fluorescence emission of QDM

As mentioned above, the fluorescence emission band of **QDM** is centered at ca. 545 nm (using samples of O.D. = 0.1 at $\lambda_{Exc} = 470$ nm) (Fig. 2). In the present study, when various equivalents of the M^{n+} analytes were added to **QDM** samples, we observed a gradual decrease in fluorescence intensity. Except for Pb^{2+} (Fig. 2e), one can clearly distinguish various degrees of change in intensity for all ions, with a distinctive selectivity for Hg^{2+} (Fig. 2d). Importantly, the decrease in the fluorescence intensity of **QDM** due to dilution was not that significant (Supplementary Information, Fig. S1). Thus, the quenching of the fluorescence can be ascribed to either energy transfer (**QDM*** \rightarrow **M**ⁿ⁺) or spin–orbit coupling (heavy atom effect) due to the nature of the metal analytes [28], particularly in the case of Hg^{2+} [29].

Out of all metal ions, $\mathbf{Hg^{2+}}$ showed stark fluorescence quenching ability upon the addition of each equivalent of the $\mathbf{HgCl_2}$ solution. As shown in Fig. 2d, the equiv of $\mathbf{Hg^{2+}}$ required for complete fluorescence quenching amounts to ca. 80 (ca. 7×10^{-4} M). We hypothesize that this higher value required for complete quenching of the fluorescence emission of **QDM** might be due to the presence of two thio-carbonyl groups in the backbone of the dye. Thus, a higher amount/concentration/equiv of $\mathbf{Hg^{2+}}$ would be required for effective and complete

complexation with **QDM**. Nevertheless, among the series of ion analytes, $\mathbf{Hg^{2+}}$ showed a higher affinity toward **QDM** (Fig. 3a). While all metal ions quench only less than 5% of the emission of **QDM** at less than 15 equiv of the $\mathbf{M^{n+}}$, it can be seen that mercury could quench ca. 85% of **QDM** fluorescence emission in a linear fashion. Beyond 25 equiv (ca. 3×10^{-4} M) of $\mathbf{Hg^{2+}}$, we observed an inflection of the curve to reach a static/saturation regime after 45 equiv To be more predictive, we zoomed our analysis onto equivalent 30 for all ions (Fig. 3b). Expectedly, one can see that **QDM** is very selective toward mercury. This result is exciting and suggests that **QDM** can be used to selectively detect mercury in a mixture of environmental pollutants.

In addition, a systematic analysis of the quenching of the fluorescence emission of **QDM** in the presence of $\mathbf{Hg^{2+}}$ was performed so that the type(s) of interactions that occurred viz. static or dynamic could be rationalized. Using Stern-Volmer (SV) quenching analysis (Fig. 3a), it was revealed that the $\mathbf{QDM/Hg^{2+}}$ interaction is dynamic up to ca. 30 equiv of $\mathbf{Hg^{2+}}$ and later changed to static quenching onwards. Focusing on the dynamic quenching regime, an SV constant $K_{SV}=3.152\times10^4$ $\mathbf{M^{-1}}$ was extracted. This value for K_{SV} translated to a rate constant K_q for quenching (or energy transfer) higher than 10^{14} $\mathbf{M^{-1}}$ s⁻¹ (with τ_{Fl} less than 100 ps). In this situation, we postulated that the high value for K_q is indicative of unimolecular or intramolecular interaction(s) since this

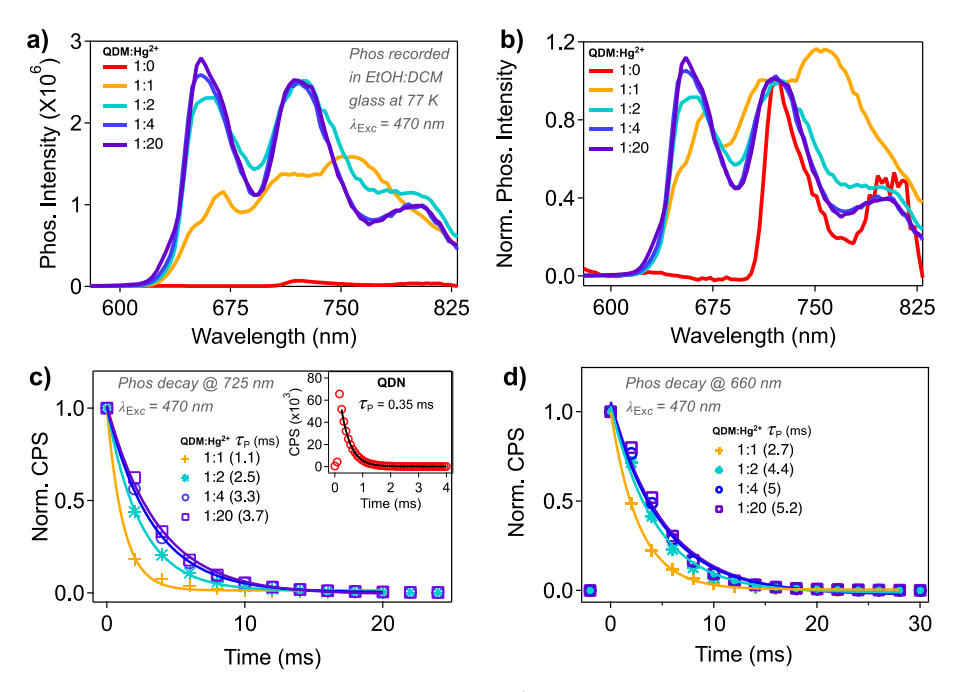


Fig. 4. (a) Phosphorescence profile of QDM in the presence of various equiv of Hg^{2+} . (b) Normalized Phosphorescence data from (a). Phosphorescence decay kinetics of QDM was monitored at (c) 725 nm and (d) 660 nm in the presence of various equiv of Hg^{2+} . Note: all phosphorescence samples (O.D. = 0.25 at 470 nm) were excited at 470 nm in EtOH/ DCM (1:1 ν/ν) glassy matrix glass at 77 K.

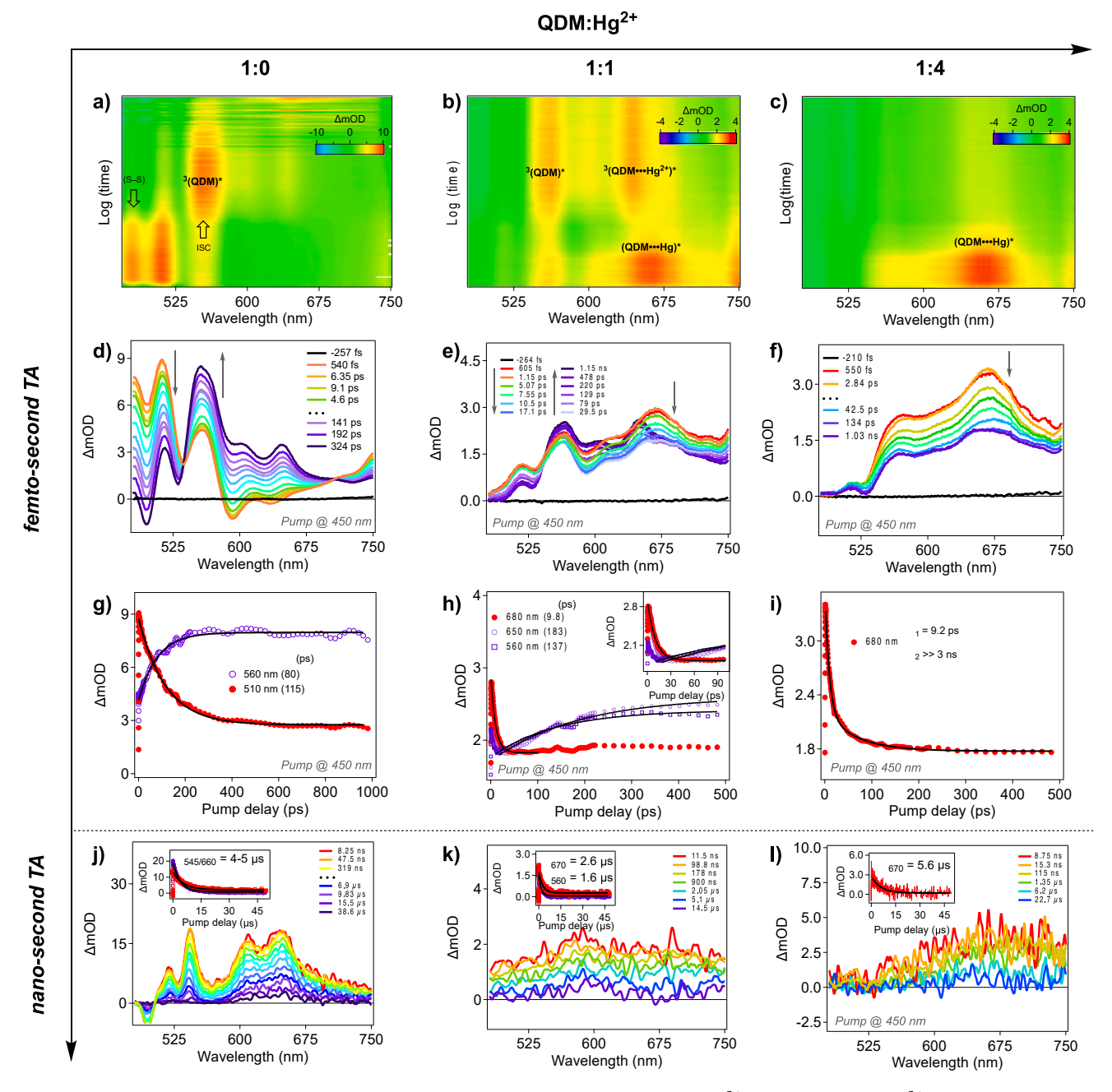


Fig. 5. Femtosecond time-resolved transient absorption 2D intensity map of (a) QDM alone, (b) QDM:Hg²⁺ (1:1), and (c) QDM:Hg²⁺ (1:4), respectively, and (d–f) their corresponding transient absorption features. (g–j) Decay kinetics traces of the transient recorded in oxygen-free ACN with samples of optical density: O.D. = 0.5 at $λ_{Exc}$ = 450 nm, 0.3 μJ/pulse and 2.5 kHz repetition rate. Nanosecond time-resolved transient absorption spectra and corresponding kinetic traces for (j) QDM alone, (k) QDM:Hg²⁺ (1:1), and (l) QDM:Hg²⁺ (1:4), respectively in oxygen-free ACN with samples of optical density: O.D. = 0.5 at $λ_{Exc}$ = 450 nm, 1 μJ/pulse and 1 kHz repetition rate.

rate is in the upper limit of the rate of molecular diffusion in solution. As shown in Scheme 1, at low concentrations of Hg^{2+} , the $QDM\cdots Hg^{2+}$ complex would exhibit a higher degree of freedom (or flexibility) highlighting the observed dynamicity. But, at higher concentrations of Hg^{2+} , the complexation would lead to a more rigid molecular complex.

For the complete understanding of the photophysics of $QDM \cdots Hg^{2+}$ interaction(s) or species, an investigation of the phosphorescence and transient absorption dynamics of samples of QDM in the presence of 0–20 equiv of Hg^{2+} was carried out.

3.3. Phosphorescence behavior of QDM/Hg²⁺ mixtures

The phosphorescence emission of various ratios of QDM:Hg²⁺

(Fig. 4) shows a significant increase of the intrinsic phosphorescence band of **QDM** upon addition of just 1 equiv of Hg^{2+} . Besides the native emission of **QDM**, centered at ca. 725 nm, new bands with λ_{max} at 660, 720, and 760 nm also appeared. As the equiv of the Hg^{2+} ion was increased from 1 to 20, the intensity of this band also increased to reach saturation at around 1:20 ratio of **QDM:** Hg^{2+} . While the phosphorescence decay kinetic at 725 nm of the emission of **QDM** alone was fitted with a mono-exponential function leading to a lifetime of 0.35 ms, decay analysis of the new band (at $\lambda_{max} = 660$ nm) in the presence of Hg^{2+} ion produced lifetime values of 2.7, 4.4, 5, and 5.2 ms for equiv of 1, 2, 4 and 20, respectively. These values are approximately one order of magnitude larger than the actual phosphorescence lifetime of **QDM** alone. This result suggests that the new $[QDM:Hg^{2+}]$ species/complex exhibits

greater stability than QDM alone in the triplet excited state.

3.4. Time-resolved pump-probe spectroscopy

To ascertain the impact of Hg^{2+} with QDM in the excited state, timeresolved pump-probe absorption spectroscopy was perfored (Fig. 5). Upon laser excitation at 450 nm, the characteristic singlet transient of **QDM** (¹**QDM***) appeared near 510 nm with a lifetime of 115 ps; then 1 1 1 1 ODM* quickly converts to the corresponding triplet transient ³QDM*at 560 nm via ISC within a time constant of 80 ps. (Fig. 5a, d). Interestingly, in the presence of 1 equiv of Hg^{2+} , the magnitude of the ¹QDM* band decreased (Fig. 5b, e) and completely disappeared at 4 equiv of Hg²⁺ (Fig. 5c, f). As shown in Fig. 5b and e, the band at 560 nm can still be ascribed to ³QDM*; but, the new band centered at 680 nm was assigned to a transient species of (QDM···Hg²⁺)* complex, presumably a charge transfer species that decayed within ca. 10 ps to yield a stable or long-lived species with charge-transfer-like features in the same spectral range (530–750 nm) (Fig. 5c, f). Also, for 1 equiv of Hg²⁺, the band at ca. 650 nm was ascribed to the triplet transient of the QDM...Hg²⁺ complex (Fig. 5h). The growth kinetics of this complex seems slower than the one of native ³**ODM***. Moreover, for 4 equiv of Hg²⁺, the optical density of (QDM...Hg²⁺* is more enhanced; this species was found to live longer than the timescale of the experiment. Hence, the band at 530-750 nm (Fig. 5c, f) was ascribed to be that of the transient of complex II (Scheme 1).

Furthermore, the triplet transients of the QDM···Hg²⁺ complex(es) for 1 and 4 equiv of Hg²⁺ were probed. In Fig. 5j, one can see that upon laser excitation at 450 nm, the characteristic absorption of the triplet transient of QDM alone appears to match the longer-timescale bands in the femtosecond transient (fs-TA) experiments (Fig. 5a,d). However, when the amount of the Hg²⁺ ion was increased (Fig. 51), these bands quickly faded and a featureless band appeared in the 525-750 nm spectral region. The kinetic trace of this band was fitted with either a mono- or bi-exponential function to give a time constant $\tau = 2.6 \text{--} 5.6~\mu s.$ This variance in the kinetic is suggestive of the presence of more than one species viz. complexes I and II. In addition it was expected that the mercury ion may also be inducing a rapid $T_1 \rightarrow S_0$ decay (via spin-orbit coupling). This effect was manifested at higher concentration of the Hg²⁺ ion (vide supra). From this analysis, one can conclude that only trace amounts of the Hg^{2+} ion would be useful in modulating the excited state of QDM (QDM)*, but at higher concentration of this ion, the formation of stable QDM···Hg²⁺ complex(es) could alter the photo-excited state behavior of **ODM**.

4. Conclusions

In summary, we showed that a sulfur-containing naphthoquinodimethyl-bis-thioamide dye (QDM), which exhibits attractive photoluminescence characteristics, can be employed as a sensor for heavy metal analytes. Among the metal analytes that were probed, it was found that **QDM** was very selective towards mercury ion (Hg^{2+}) which quenched more than 85% of the fluorescence band of QDM at ca 30 equiv. This investigation also established that the strong QDM...Hg²⁺ interaction(s) led to quenching of the fluorescence of the sensor with kinetics near or beyond molecular diffusion limit. This result prompted us to investigate the photophysics of the sensor...analyte complex and/or interaction(s) using matrix isolation and time-resolved pump-probe spectroscopy techniques. While a lower concentration (ca. 1×10^{-5} M) of Hg²⁺ ions was found to modulate the photo-excited state behavior of the QDM dye, it was ascertained that a concentration from 4 equiv (ca. 1×10^{-4} M) of Hg^{2+} is sufficient to form stable QDM \cdots Hg²⁺ complex(es). The present work highlights the use of organic dyes, that exhibit low structural complexities, as valuable chemical sensors for environmental pollutants. Ongoing derivatization/functionalization with QDM and its analogues will help in increasing the sensitivity in the present investigation.

5. Funding sources

National Science Foundation under a CAREER grant no. 1,753,012 Awarded to AJA.

Illinois Tech Graduate Kilpatrick and Starr Fieldhouse Fellowships to $\mathbf{v}_{\mathbf{I}\mathbf{Y}}$

The Organization for women in science for the Developing World (OWSD) Fellowship to VOA.

Declaration of Competing Interest

The authors declare that they have no known competing financial interests or personal relationships that could have appeared to influence the work reported in this paper.

Acknowledgments

This material is based upon work supported by the National Science Foundation under a CAREER grant no. 1753012 Awarded to AJA. SM and AJA are grateful for the financial support from the Illinois Tech Educational and Research Initiate Fund. YJY is thankful for the support from the Kilpatrick Graduate Fellowship and the Starr Fieldhouse Research Fellowship Programs at Illinois Tech. VAO thanks the generous support from the OWSD Fellowship Program. Use of the Center for Nanoscale Materials, an Office of the Science user facility, was supported by the U.S. Department of Energy, Office of Science, Office of Basic Energy Science, under Contract No. DE-AC02-06CH11357.

Appendix A. Supplementary data

Additional UV-vis absorption spectra, emission spectra, and NMR titration data. Supplementary data to this article can be found online at https://doi.org/10.1016/j.jphotochem.2021.113648.

References

- P.B. Tchounwou, C.G. Yedjou, A.K. Patlolla, D.J. Sutton, Molecular, clinical and environmental toxicology, volume 3: environmental toxicology, Exp. Suppl. 101 (2012) 133–164, https://doi.org/10.1007/978-3-7643-8340-4_6.
- [2] P. Li, X.B. Feng, G.L. Qiu, L.H. Shang, Z.G. Li, Mercury pollution in asia: a review of the contaminated sites, J. Hazard. Mater. 168 (2-3) (2009) 591–601, https://doi. org/10.1016/j.jhazmat.2009.03.031.
- [3] R. Dghaim, S.A. Khatib, H. Rasool, M.A. Khan, Determination of heavy metals concentration in traditional herbs commonly consumed in the united Arab emirates, J. Environ. Public Heal 2015 (2015) 1–6, https://doi.org/10.1155/2015/ 973878.
- [4] J.-J. Kim, Y.-S. Kim, V. Kumar, Heavy metal toxicity: an update of chelating therapeutic strategies, J. Trace Elem Med. Biol. 54 (2019) 226–231, https://doi. org/10.1016/j.jtemb.2019.05.003.
- [5] R. Schoeny, Use of genetic toxicology data in U.S. EPA risk assessment: the mercury study report as an example, Environ Health Persp 104 (suppl 3) (1996) 663–673, https://doi.org/10.1289/ehp.96104s3663.
- [6] Dhillon, G.; Health, B. S. of H. S., Environmental; Heacock, H.; Afshari, R. Blood Concentrations of Lead and Mercury in British Columbians (2009-2010). *Bcit Environ Public Heal J* 2016. https://doi.org/10.47339/ephj.2016.95.
- [7] C.-E. Ai, C.-J. Li, M.-C. Tsou, J.-L. Chen, H.-C. Hsi, L.-C. Chien, Blood and seminal plasma mercury levels and predatory fish intake in relation to low semen quality, Environ. Sci. Pollut. R 26 (19) (2019) 19425–19433, https://doi.org/10.1007/ s11356-019-04592-6.
- [8] K.A. Graeme, C.V. Pollack, Heavy metal toxicity, Part I: arsenic and mercury,
 J. Emerg. Med. 16 (1) (1998) 45–56, https://doi.org/10.1016/S0736-4679(97)
- [9] N. Langford, R. Ferner, Toxicity of mercury, J. Hum. Hypertens. 13 (10) (1999) 651–656, https://doi.org/10.1038/sj.jhh.1000896.
- [10] Sabiha-Javied, T. Mehmood, M.M. Chaudhry, M. Tufail, N. Irfan, Heavy metal pollution from phosphate rock used for the production of fertilizer in Pakistan, Microchem. J. 91 (1) (2009) 94–99, https://doi.org/10.1016/j. microc.2008.08.009.
- [11] J.W. Lim, T.-Y. Kim, M.-A. Woo, Trends in sensor development toward next-generation point-of-care testing for mercury, Biosens. Bioelectron. 183 (2021) 113228, https://doi.org/10.1016/j.bios.2021.113228.
- [12] M.Y. Burylin, K.A. Romanovskiy, Z.A. Temerdashev, E.F. Galai, Determination of mercury in sediments by slurry sampling electrothermal atomic absorption spectrometry, J. Anal. Chem. 74 (12) (2019) 1184–1191, https://doi.org/10.1134/ s1061934819120037.

- [13] M.J. Gismera, D. Hueso, J.R. Procopio, M.T. Sevilla, Ion-selective carbon paste electrode based on tetraethyl thiuram disulfide for copper(II) and mercury(II), Anal. Chim. Acta 524 (1–2) (2004) 347–353, https://doi.org/10.1016/j. aca.2004.03.098.
- [14] M. Fialin, H. Remy, C. Richard, C. Wagner, Trace element analysis with the electron microprobe; New data and perspectives, Am. Mineral 84 (1–2) (1999) 70–77, https://doi.org/10.2138/am-1999-1-207.
- [15] F.Y. Lee, J.A. Kittrick, Electron microprobe analysis of elements associated with zinc and copper in an oxidizing and an anaerobic soil environment, Soil Sci. Soc. Am. J. 48 (3) (1984) 548–554, https://doi.org/10.2136/ sssai1984.03615995004800030016x.
- [16] M.S. Rahman, S.M. Hossain, M.T. Rahman, M.A. Halim, M.N. Ishtiak, M. Kabir, Determination of trace metal concentration in compost, DAP, and TSP fertilizers by neutron activation analysis (NAA) and insights from density functional theory calculations, Environ. Monit. Assess. 189 (12) (2017) 618, https://doi.org/ 10.1007/s10661-017-6328-1.
- [17] B. Valeur, I. Leray, Design principles of fluorescent molecular sensors for cation recognition, Coordin. Chem. Rev. 205 (1) (2000) 3–40, https://doi.org/10.1016/ s0010-8545(00)00246-0.
- [18] S. Shokri, J. Li, M.K. Manna, G.P. Wiederrecht, D.J. Gosztola, A. Ugrinov, S. Jockusch, A.Y. Rogachev, A.-L. Ayitou, A Naphtho- p-quinodimethane exhibiting baird's (Anti)Aromaticity, broken symmetry, and attractive photoluminescence, J. Organ. Chem. 82 (19) (2017) 10167–10173, https://doi.org/10.1021/acs. ioc.7b01647
- [19] S. Shokri, G.P. Wiederrecht, D.J. Gosztola, A.-L. Ayitou, Photon upconversion using baird-type (Anti)aromatic quinoidal naphthalene derivative as a sensitizer, J. Phys. Chem. C 121 (42) (2017) 23377–23382, https://doi.org/10.1021/acs. ipcc.7b08373.
- [20] J. Morgan, Y.J. Yun, A.-J.-L. Ayitou, Estimation of singlet oxygen quantum yield using novel green-absorbing baird-type aromatic photosensitizers, Photochem. Photobiol. (2021), https://doi.org/10.1111/php.13483.

- [21] R.G. Pearson, Hard and soft acids and Bases, HSAB, part 1: fundamental principles, J. Chem. Educ. 45 (9) (1968) 581, https://doi.org/10.1021/ed045p581.
- [22] X. Zhang, X.-J. Huang, Z.-J. Zhu, A Reversible Hg(ii)-selective fluorescent chemosensor based on a thioether linked bis-rhodamine, RSC Adv. 3 (47) (2013) 24891–24895, https://doi.org/10.1039/c3ra43675f.
- [23] N. Manav, P.E. Kesavan, M. Ishida, S. Mori, Y. Yasutake, S. Fukatsu, H. Furuta, I. Gupta, Phosphorescent rhenium-dipyrrinates: efficient photosensitizers for singlet oxygen generation, Dalton Trans. 48 (7) (2019) 2467–2478, https://doi. org/10.1039/c8dt04540b.
- [24] M. Ponram, U. Balijapalli, B. Sambath, S.K. Iyer, V. B, R. Cingaram, K. Natesan Sundaramurthy, Development of paper-based chemosensor for the detection of mercury ions using mono- and tetra-sulfur bearing phenanthridines, New J. Chem. 42 (11) (2018) 8530–8536, https://doi.org/10.1039/C8NJ00760H.
- [25] M. Vasak, J.H.R. Kaegi, H.A.O. Hill, Zinc(II), cadmium(II), and mercury(II) thiolate transitions in metallothionein, Biochemistry-US 20 (10) (1981) 2852–2856.
- [26] B.P. Kennedy, A.B.P. Lever, Studies of the metal-sulfur bond. Complexes of the pyridine thiols, Can. J. Chem. 50 (21) (1972) 3488–3507, https://doi.org/ 10.1139/v72-563
- [27] D.A. Pardo-Rodriguez, J.J. Mendez, S.M. Mejía, Computational characterization of organic ligands derived from fumaric acid for selective adsorption of inorganic mercury, Inform. Tecnol. 31 (2) (2020) 81–92, https://doi.org/10.4067/s0718-07642020000200081.
- [28] R.F. Chen, Phosphorescence of tryptophan and proteins in the presence of silver ion, Arch. Biochem. Biophys. 166 (2) (1975) 584–591, https://doi.org/10.1016/ 0003-9861(75)90423-3
- [29] H. Kunkely, O. Horváth, A. Vogler, Photophysics and photochemistry of mercury complexes, Coordin. Chem. Rev. 159 (1997) 85–93, https://doi.org/10.1016/ s0010-8545(96)01307-0.